

## Supplementary information

for

### Effects of structural differences between $\gamma$ -MnO<sub>2</sub> and $\gamma$ -Mn<sub>2</sub>O<sub>3</sub> catalysts on CO oxidation: different active oxygen species and carbonate species using *operando* TPR-DRIFTS-MS

Jiacheng Xu<sup>1,3\*</sup>, Peng Weng<sup>2</sup>, Shuiliang Yao<sup>3,4\*</sup>

<sup>1</sup> School of Ceramics, Wuxi Vocational Institute of Arts & Technology, Yixing 214206, China

<sup>2</sup> Changzhou University Huaide College, JingJiang Jiangsu 214500, China

<sup>3</sup> School of Environmental Science and Engineering, Changzhou University, Changzhou 213164, China

<sup>4</sup> Key Laboratory of Advanced Plasma Catalysis Engineering for China Petrochemical Industry, Changzhou, China

\*Corresponding author. Email: [xujiacheng628@163.com](mailto:xujiacheng628@163.com) and [yaos@cczu.edu.cn](mailto:yaos@cczu.edu.cn)

#### S1. Supplementary information

##### S1.1. Catalyst preparation

$\gamma$ -MnO<sub>2</sub> and  $\gamma$ -Mn<sub>2</sub>O<sub>3</sub> is prepared by aerosol method, the specific steps are as follows: The manganese nitrate solution (Mn(NO<sub>3</sub>)<sub>2</sub>, 50 wt.% in H<sub>2</sub>O, Aladdin Shanghai, China) is added to the deionized water to make the total amount reach 50 mL. After mixing thoroughly, the solution is placed into a Pyrex bottle (500 mL) containing an ultrasonic atomizer (ZP-01, Chenyang Electric, China). The atomized fog is mixed with 1 L min<sup>-1</sup> N<sub>2</sub> air flow and passed through a tube preheated to 70°C to enhance the vaporization of water in the nitrate fog to form a nitrate aerosol. Air streams carrying nitrate aerosols are then directed into quartz tubes where they undergo high-temperature decomposition at 600°C ( $\gamma$ -Mn<sub>2</sub>O<sub>3</sub>) or 400°C ( $\gamma$ -MnO<sub>2</sub>). The particles produced by nitrate decomposition are collected by a two-stage adsorber. The collected hydrocolloid is transferred to a centrifuge tube and centrifuged at 10000 rpm for 3 min to obtain solid precipitation. The solid sediment is washed with deionized water and ethanol for 2 to 3 times, and then dried in an oven at 80°C for 12 h, and the dry solid sample obtained is named  $\gamma$ -Mn<sub>2</sub>O<sub>3</sub>.

##### S1.2. Catalyst characterization

The crystal form and crystallinity of the catalyst were determined by XRD (Rigaku Ultimate

IV type, Rigaku, Japan) operated at 40 mA, 40 kV, 10~80°, and 5 °/min.

X-ray photoelectron spectroscopy (XPS, Thermo Scientific K-Alpha, Thermo Fisher Scientific, USA) was used to measure element distribution and oxidation states on the catalyst surfaces under conditions: Al K $\alpha$  ray:  $h\nu=1486.6$  eV, beam spot: 400  $\mu\text{m}$ , chamber vacuum: better than  $5.0\text{E-}7$  mBar, working voltage: 12 kV, filament current: 6 mA.

A fully automatic specific surface and porosity analyzer (Micromeritics ASAP2460, Micromeritics, USA) was used to measure the specific surface areas, pore diameters, and pore volumes. All catalyst samples were dried at 150°C for 6 h, degassed at 300°C for 8 h. Brunauer-Emmett-Teller (BET) was used to calculate specific surface areas of the catalysts. The pore diameter and pore volume of the samples were determined using Barrett-Joyner-Halenda (BJH) calculation.

The surface morphologies of the catalysts were observed using a scanning electron microscope (SEM, Hitachi Regulus 8100, Hitachi, Japan) with a SE2 secondary electron detector. The lattice stripes and elements distribution on the catalyst surfaces were detected with a high-resolution electric field emission transmission electron microscope (HRTEM, FEITecnaiF20, USA).

Characterized the oxygen vacancy information of materials using Electron Paramagnetic Resonance (EPR, Germany, Bruker A300). A small sample was placed in a capillary tube for measurement at room temperature. The X-band frequency employed was 9.82 GHz.

### 1.3 Catalyst evaluation

The CO oxidation rate ( $r_{CO}$ ,  $\mu\text{mol}\cdot\text{min}^{-1}\cdot\text{m}^{-2}$ ) was calculated based on BET surface area using Eq. S1.

$$r_{CO} = \frac{[CO]_{in} \times X_{CO} \times V_{gas}}{m_{cat} \times S_{BET}}$$

(S1)

where,  $[CO]_{in}$  and  $X_{CO}$  are CO concentration ( $\mu\text{mol L}^{-1}$ ) in the gas at the inlet of the fixed-bed quartz tubular reactor and CO conversion, respectively.  $V_{gas}$  is the gas flow rate in  $\text{L min}^{-1}$ .  $m_{cat}$  is the quantity of the catalyst in mg.  $S_{BET}$  is the BET surface area in  $\text{m}^2 \text{mg}^{-1}$ .

The activation energy ( $E_a$ ,  $\text{kJ mol}^{-1}$ ) of CO oxidation was calculated based on the Arrhenius equation, on the condition of  $X_{CO}$  lower than 20% [2, 3]:

$$\ln r_{CO} = -\frac{E_a}{RT} + \ln A \quad (\text{S2})$$

## Reference:

- [1] M.C. Biesinger, B.P. Payne, A.P. Grosvenor, L.W.M. Laua, A.R. Gerson, R.S.C. Smart, Resolving surface chemical states in XPS analysis of first row transition metals, oxides and hydroxides: Cr, Mn, Fe, Co and Ni. *Appl. Surf. Sci.* 257 (2024) 2717-2730.
- [2] A. Jia, G. Hu, L. Meng, et al. CO oxidation over  $\text{CuO/Ce}_{1-x}\text{Cu}_x\text{O}_{2-\delta}$  and  $\text{Ce}_{1-x}\text{Cu}_x\text{O}_{2-\delta}$  catalysts: Synergetic effects and kinetic study. *J. Catal.* 289 (2012) 199-209.
- [3] J. Qing, C. Sun, N. Li, et al. Kinetic study of CO oxidation over  $\text{CuO/MO}_2$  ( $\text{M} = \text{Si, Ti and Ce}$ ) catalysts. *Appl. Surf. Sci.* 287 (2023) 124-134.

## S2. Figures

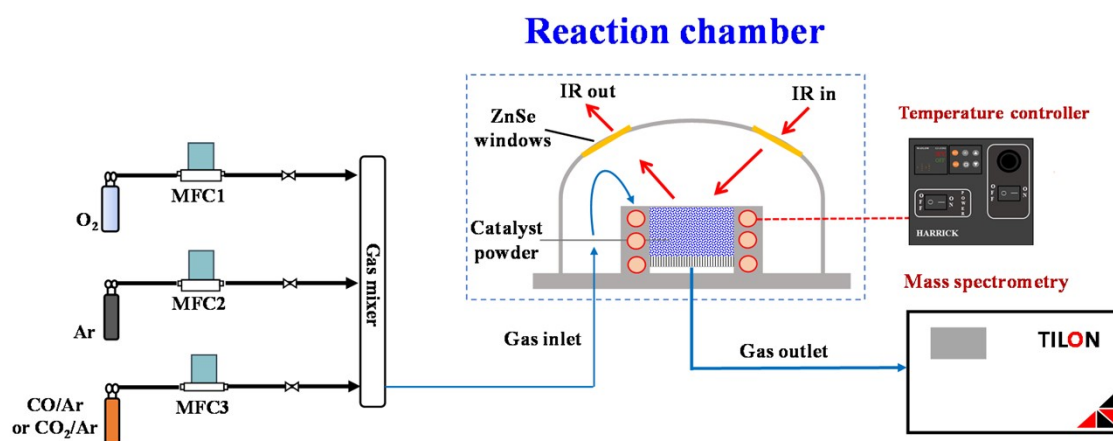
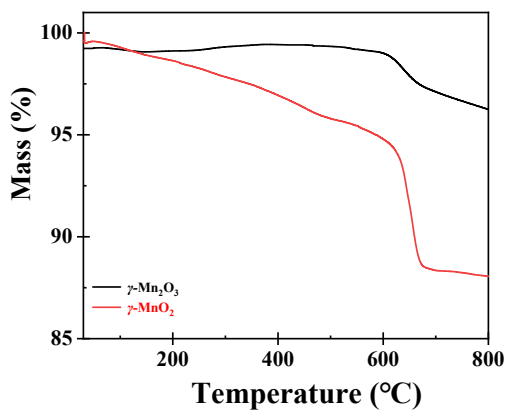


Figure.S1. Experimental setup of the *operando* TPR-DRIFTS-MS system.

In order to further confirm the source of type III oxygen in O<sub>2</sub>-TPD (above 600°C). TG experiments are performed on  $\gamma$ -MnO<sub>2</sub> and  $\gamma$ -Mn<sub>2</sub>O<sub>3</sub> catalysts (Figure. S2). The mass of  $\gamma$ -Mn<sub>2</sub>O<sub>3</sub> catalyst does not change before 600°C. When the temperature reached above 600°C, the mass decreased significantly, indicating that the structure of  $\gamma$ -Mn<sub>2</sub>O<sub>3</sub> catalyst changed. This process is mainly the process of Mn<sub>2</sub>O<sub>3</sub> (Mn<sup>3+</sup>) to change MnO (Mn<sup>2+</sup>). However, the mass of  $\gamma$ -MnO<sub>2</sub> catalyst begins to decline from 50°C. There are three main stages of mass decline. The first stage is below 200°C, and this stage may be due to the removal of adsorbed water or impurities on the catalyst surface. The second stage is 200°C-600°C, which is mainly caused by the loss of surface lattice oxygen of MnO<sub>2</sub> (Mn<sup>4+</sup>) to Mn<sub>2</sub>O<sub>3</sub> (Mn<sup>3+</sup>). The third stage is higher than 600°C, which is consistent with  $\gamma$ -Mn<sub>2</sub>O<sub>3</sub> catalyst.



**Figure S2.** TGA diagrams of  $\gamma$ -MnO<sub>2</sub> and  $\gamma$ -Mn<sub>2</sub>O<sub>3</sub> catalysts.

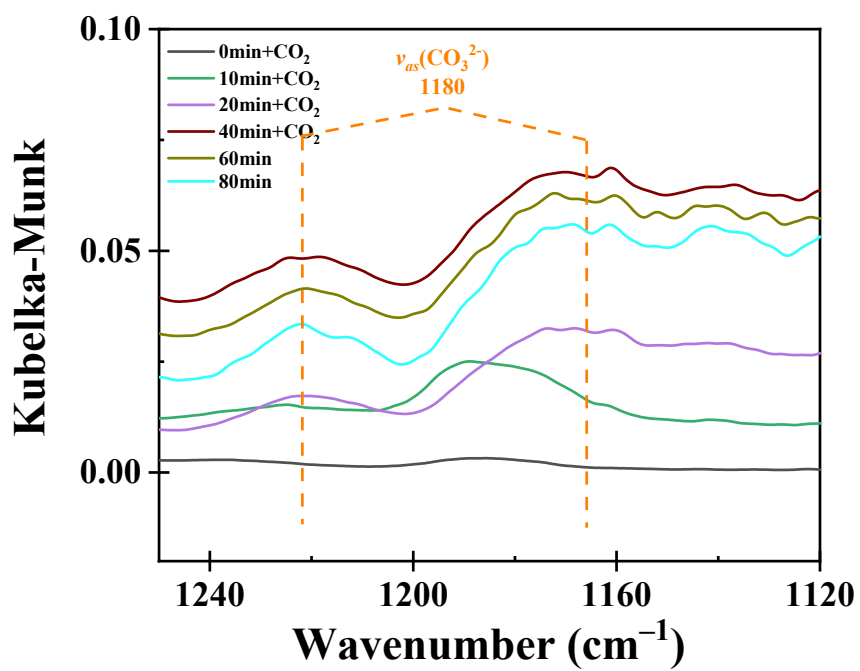
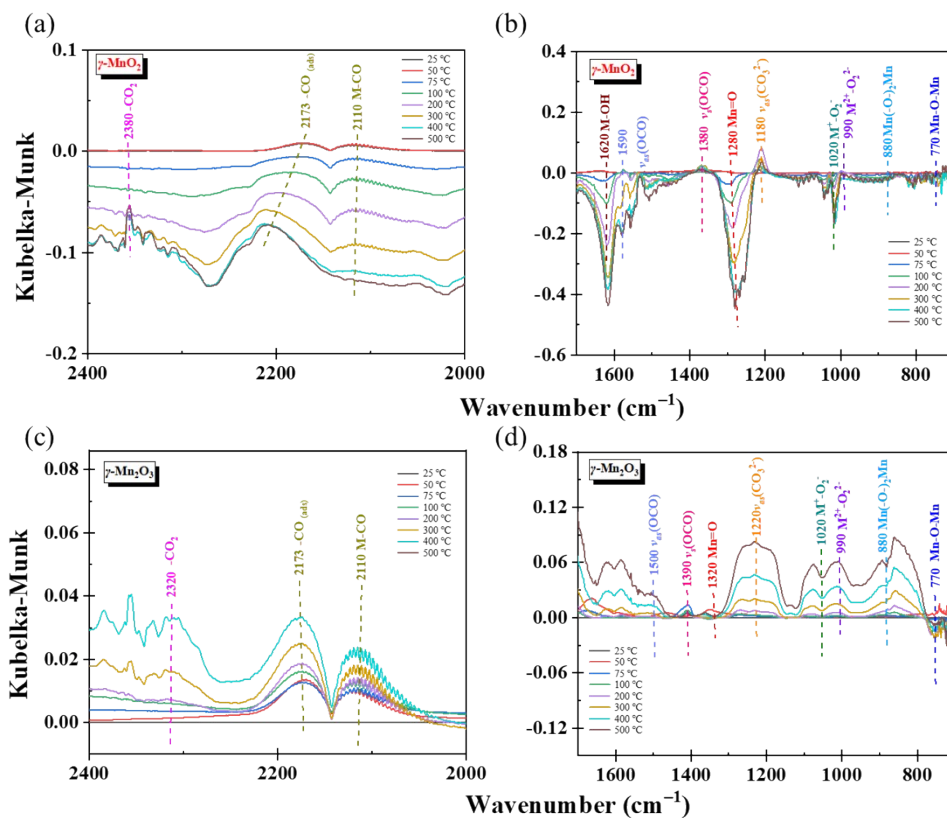
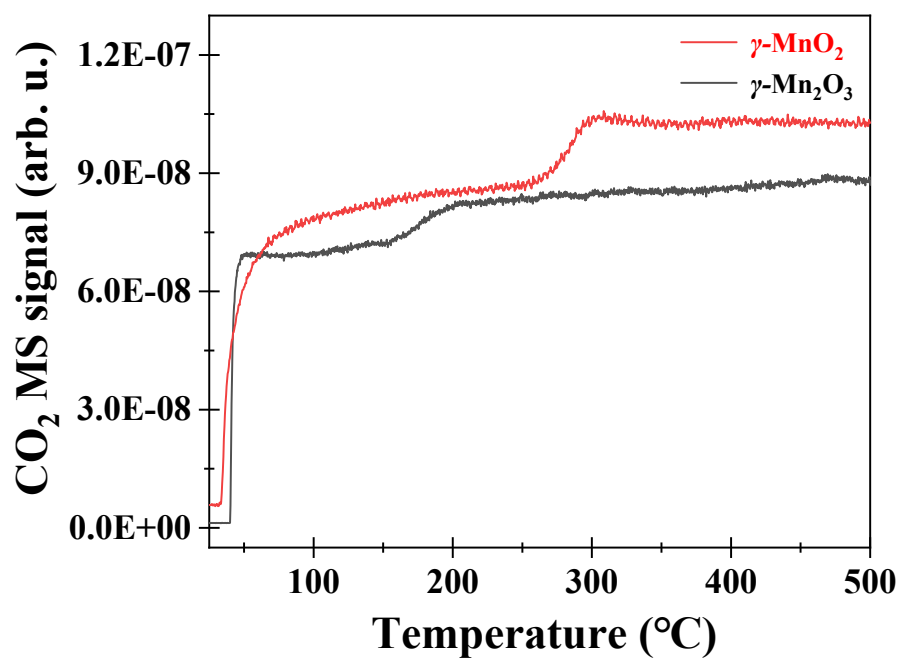


Figure.S3. DRIFTS spectra of  $\gamma$ -MnO<sub>2</sub> under CO/Ar atmospheres at different time.



**Figure S4.** DRIFTS spectra of different  $\text{MnO}_2$  catalysts under  $\text{CO}+\text{O}_2/\text{Ar}$  atmospheres at different temperatures.



**Figure S5.** CO<sub>2</sub>MS signal of different MnO<sub>2</sub> catalysts under CO+O<sub>2</sub>/Ar atmospheres at different temperatures.

**Table S1** Composition of the gases fed to the reaction chamber.

Gas atmosphere	Composition (%)	Total gas flow rate (mL/min)
CO/Ar	CO: 2.37%, Ar: balance	38
CO+O <sub>2</sub> /Ar	CO: 2.37%, O <sub>2</sub> :10%, Ar: balance	38
CO <sub>2</sub> /Ar	CO <sub>2</sub> : 2.37%, Ar: balance	38